IEEE Access
Multidisciplinary | Rapid Review | Open Access Journal

Received May 29, 2020, accepted July 6, 2020, date of publication August 5, 2020, date of current version April 8, 2021.

*Digital Object Identifier 10.1109/ACCESS.2020.3011629*

# Research on Power Matching and Energy Optimal Control of Active Load-Sensitive Electro-Hydrostatic Actuator

**LIGANG HUANG, TIAN YU, (Member, IEEE), ZONGXIA JIAO, (Senior Member, IEEE), AND YANPENG LI**

School of Automation Science and Electrical Engineering, Beihang University, Beijing 100191, China

Corresponding author: Ligang Huang (huangligang_111@buaa.edu.cn)

This work was supported in part by the National Natural Science Foundation of China through the Major Program under Grant 51890882, and in part by the National Program on Key Basic Research Project under Grant 2014CB046400.

**ABSTRACT** Electro-hydrostatic actuator (EHA) is an important type of power-by-wire (PBW) which is a highly integrated closed volume control system with the advantages of high reliability, high efficiency and easy maintenance. However, under heavy load conditions, a large amount of heat the EHA motor produces affects the system's working time and even the system life, which restricts the widespread application of EHA systems. In order to solve the problem of motor heating and the contradiction between high dynamics and high efficiency of the EHA system, a novel active load-sensitive principle and structure of EHA system is proposed based on the load-sensitive principle. The active load-sensitive EHA (ALS-EHA) is a dual control variable system consisting of a motor pump main loop and a load-sensitive loop. As for the latter, the system load pressure is introduced into a special designed and optimized pressure fellow valve (PFV). The valve outlet is connected to the plunger pump swash plate variable mechanism. The EHA pump displacement is actively adjusted by controlling the current input to PFV. The two-degree-of-freedom cooperative control for the output flow of the pump can be implemented by adjusting the motor speed and the pump displacement. An energy optimal robust control law based on fuzzy and disturbance compensation is presented for the control architecture. The simulation results show that the ALS-EHA system based on the control law proposed in this paper can effectively reduce the motor heat while ensuring the dynamic performance of the system.

**INDEX TERMS** Active load-sensitive, electro-hydrostatic actuator, fuzzy control, optimal efficiency, power matching.

## I. INTRODUCTION

With the emerging development of More/All-Electric-Aircraft (MEA/AEA), PBW has become the spread trend of flight control actuation system, which has attracted extensive attention and research [1]–[4]. MEA/AEA refers to the use of electrical energy to replace mechanical, hydraulic and other transmission methods to achieve aircraft energy transmission and signal transmission to various subsystems. PBW replaces the hydraulic pipelines with power cables to achieve the power transmission function of the aircraft in the form of electrical energy transmission. This will eliminate the dual secondary energy structure that has both a power source and a hydraulic source on the aircraft so that making the aircraft more flexible. It has absolute advantages in many aspects such as reliability, volume quality, system layout design, maintainability and economy [5]–[7]. Electro-Hydrostatic Actuator (EHA) is an important type of PBW [8]. The EHA system usually consists of a controller, a motor, a hydraulic pump, an integrated valve block, an actuator, and hydraulic valve elements. It is a multi-disciplinary system of mechanical, electrical, hydraulic, thermal control with complex model and strong nonlinearity. It adjusts the system flow by controlling either the motor speed or the pump displacement to control the movement of the actuator [8]. From the perspective of motors and pumps, there are three main forms of EHA systems [9]: The first is variable displacement-constant speed EHA (Variable Pump Displacement, Fixed Motor Speed and VPFM), that is, the motor speed is kept constant, and the system flow is adjusted by changing the

The associate editor coordinating the review of this manuscript and approving it for publication was Yingxiang Liu.

displacement of the variable pump to achieve system servo control. This type has simple structure, but it has low system efficiency and low control accuracy [10]. The second type is fixed displacement-variable speed EHA (Fixed Pump Displacement, Variable Motor Speed and FPVM), that is, the displacement of the pump remains unchanged, and the system flow is adjusted by controlling the speed of the motor to achieve system servo control. This structure is simple to control, but there is a dead zone at the zero crossing of the motor speed, which affects the accuracy and stability of the system. In addition, the motor generates severe heat under low speed and heavy load conditions, and cannot achieve power matching in the full range of operating conditions. The third is variable displacement-variable speed EHA (Variable Pump Displacement and Variable Motor Speed, VPVM), that is, the speed of the motor and the displacement of the pump are both variable. The traditional architecture of this type has high efficiency and good dynamic characteristics. Dual variable control can realize the power matching of the system, but the control architecture is complex and requires a variable mechanism. The hydraulic variable mechanism requires an additional set of hydraulic energy. Therefore, the variable mechanism of the ball screw driven by an electric drive has appeared, but the mechanical transmission is not high in accuracy and has problems such as backlash etc.

The EHA system has a series of advantages of PBW, but the contradiction between its dynamic performance and motor heating has always puzzled researchers in various countries around the world, and has become the main reason affecting its wide application [8], [9]. How to implement the EHA with high power density, high efficiency and high dynamic performance is the main problem that scholars need to solve urgently [10]. At present, there are several solutions to the problem of EHA heating. One is to use a high-pressure and high-speed method to increase the system pressure to 35 MPa and the speed to above 15000 rpm to reduce the output torque of the motor and the heat generation [11]–[15]. This method has been applied in companies such as LIEBHERR, UTC-Goodrich, Safran-Messier-Bugatti, but the problems of friction torque and surface wear caused by high speed have extremely high requirements for structural design and processing technology, and have a great impact on system life [12], [16]–[19]. The second is to adopt a dual-variable EHA structure. By designing a reasonable control law, the system's power matching is implemented to solve the contradiction between dynamic performance and efficiency of the system. The second is the use of a dual-variable EHA structure. The system's power matching is achieved by designing reasonable control laws to solve the contradiction between dynamic performance and efficiency. However, the conventional one requires an independent hydraulic system or an electric drive system to control the pump displacement, as well the external additional hydraulic energy, motor and other accessories increase the volume and quality of the system [20]–[25].

In response to the above situation, Professor Jiao proposed the pioneering principle of load-sensitive EHA including direct load sensitivity and active load sensitivity. The former directly introduces the load pressure into the variable mechanism of the pump, and the gradient of displacement to load pressure is constant [26]. Therefore, in order to solve the system instability caused by the large displacement gradient, the stiffness of the compressed spring needs to be sufficiently large, which limits the adjustable range of pump displacement and system dynamic performance [25]. The latter is that the system load pressure is introduced into a specially designed FPV, of which outlet is connected to the plunger pump swash plate variable mechanism. The current input to valve can actively adjust the EHA pump displacement, thereby achieving the better power matching of the system. Its displacement gradient is adjustable, so the stiffness of the back pressure spring can be chosen very small, which increases the adjustment range of the displacement and the system dynamics. This is a novel principle and structure of dual-variable EHA system, which effectively solves the contradiction between high dynamics and high efficiency of the system. Furthermore, ALS-EHA does not require an independent power source to change the pump displacement, which completely reduces the burden on volume and quality caused by independent power supply.

The structure of this paper is as follows: section 2 introduces and further develops the load sensitivity principle and the FPV principle; section 3 conducts detailed modeling and analysis of the system; section 4 proposes the control law of the system; section 5 simulation and experimental verification. Finally conclusion.

## II. PRINCIPLE

To enhance the dynamic performance of the Direct Load-Sensitive (DLS), as well as taking the motor heating into accounts, the concept and principle of ALS are proposed. The key point of ALS is that a special pressure control valve is installed between the Load-Sensitive pressure port and the actuator of the swash plate in the Load Sensitive pump. It is possible to actively control the Load-Sensitive pressure by controlling the special valve named the PFV. The structure schematic diagram of ALS is shown in Fig 1.

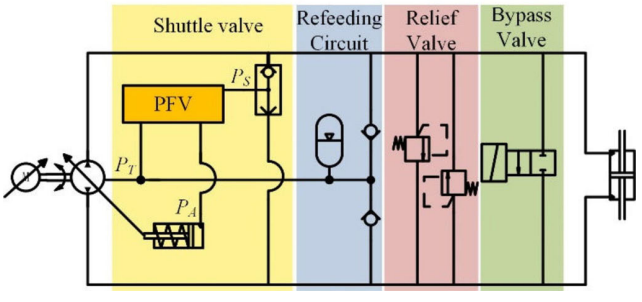


**FIGURE 1.** The structure schematic diagram of ALS.

The main components of ALS include servo motor, Load Sensitive pump, dual symmetrical hydraulic actuator, shuttle valve, PFV and other hydraulic auxiliary components. The shuttle valve is used to identify the direction of the load pressure acting on the servo variable mechanism actuator of the hydraulic pump. Besides, it will maintain the operating state of the Load-Sensitive mechanism when the direction of the load force is changed. The PFV can control the pressure acting on the Load Sensitive pump through the external control signal. The single acting hydraulic actuator is the main component of the Load Sensitive pump, which is used to change the swash plate angle of the hydraulic pump according to the output pressure of the valve. The ALS virtual prototype is shown in Fig 2.

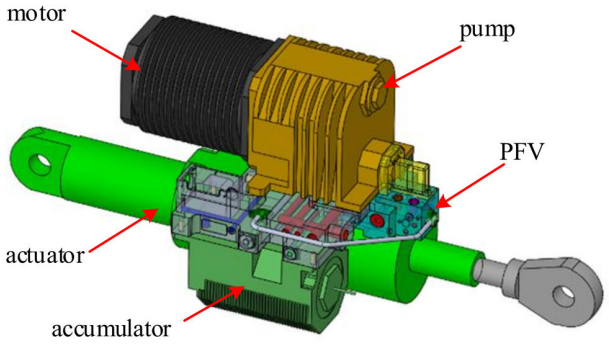


**FIGURE 2.** The virtual prototype of the ALS.

### A. PRINCIPLE OF PFV

The PFV is the main component to achieve the active control of Load-Sensitive EHA. The structure schematic of the PFV is shown in Fig. 3. The supply pressure of the PFV is the load pressure of the EHA system. The outlet pressure of PFV acts on the variable mechanism of the Load Sensitive pump to control the displacement of the pump. The return port of the valve is connected to the charge accumulator of the EHA system, which is used to reduce the outlet pressure when the outlet pressure is connected to the return port. The proportional solenoid is adopted to drive the spool directly, and the return spring can push the spool to its original position, which can enhance the stiffness and the dynamic characteristic of the valve. In order to reduce the output force of the proportional solenoid, there are two hydraulic half bridges set at the inlet and outlet of the valve respectively to reduce the feedback pressure. The reliability of the mechanical structure is greater than that of the electronic device. The working principle of the PFV is shown in Fig 3.

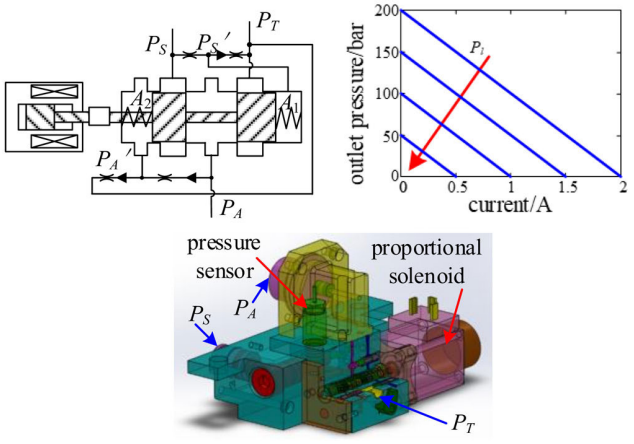


**FIGURE 3.** The schematic and virtual prototype of PFV.

The outlet pressure of the PFV can be controlled by the proportional solenoid and changes with the inlet pressure. The use of PFV cancel the demand of additional power source, which enhance the specific power of the system compared with the traditional VPVM. According to the system principle of the PFV, the virtual prototype of the PFV is designed, as shown in Fig 3.

## III. EFFICIENCY AND DYNAMIC ANALYSIS

In order to accurately understand the performance characteristics of the ALS-EHA system, this section conducts an in-depth mathematical analysis of the system's efficiency.

### A. EFFICIENCY ANALYSIS

To analyze the efficiency of the system, it is necessary to analyze it from the following parts: motor, plunger pump, actuator, valve-controlled hydraulic assembly.

The main parameters of the motor and pump for the designed EHA are shown in Table 1.

**TABLE 1.** The main parameters for the motor and pump.

| Symbol | Quantity | Value |
|---|---|---|
| $R_m$ | total armature resistance | 0.36 Ω |
| $K_e$ | motor back-EMF constant | 0.23 Vs/rad |
| $J_m$ | equivalent total motor inertia | 8.8×10-4 Kgm$^2$ |
| $J_p$ | equivalent pump total inertia | 4.2×10-4 Kgm$^2$ |
| E | power voltage | 270 V |
| $I_m$ | motor rated current | 45 A |
| $L_m$ | armature inductance | 1.7×10-3 H |
| $K_t$ | motor torque constant | 0.23 Nm/A |
| $B_m$ | equivalent total damping coefficient | 2×10-3 Nm/(rad/s) |
| $\omega_{max}$ | no-load maximum speed | 1047 rad/s |
| $P_E$ | power | 15 kW |
| $T_m$ | peak output torque | 20Nm |

#### 1) MOTOR

Stator current and resistance are the main parameters that affect the efficiency of brushless DC motors. Almost all the power loss of the motor is converted into heat [27].

$$\Delta Q_{mw} = i_s^2 R_m [1 + \sigma (G_m - G_{m0})] + k_i \omega^2 \quad (1)$$

where, the first and second terms are winding copper loss and stator iron loss, respectively. Where $i_s$ is the average current in the stator winding, $k_i$ is the proportionality factor, $G_{m0}$ and

$G_m$ are the initial temperature and the operating temperature of the motor, respectively, and $\sigma$ is the temperature compensation coefficients of the winding resistance.

The total motor power can be expressed as

$$P_e = K_t i_s \omega + \Delta Q_{mw} \tag{2}$$

where, $K_t$ is the torque constant. The motor efficiency on copper loss and iron loss can be expressed as

$$\begin{aligned}\eta_{\mathrm{m1}} &= 1 - \frac{\Delta Q_{\mathrm{mw}}}{P_{\mathrm{e}}} \\ &= 1 - \frac{i_{\mathrm{s}}^2 R_{\mathrm{m}} \left(1 + \sigma \, \Delta G_{\mathrm{m}}\right) + k_{\mathrm{i}} \omega^2}{K_t i_{\mathrm{s}} \omega + i_{\mathrm{s}}^2 R_{\mathrm{m}} \left(1 + \sigma \, \Delta G_{\mathrm{m}}\right) + k_{\mathrm{i}} \omega^2}\end{aligned} \tag{3}$$

The mechanical efficiency of the motor is shown as

$$\eta_{m2} = \frac{T_p}{T_p + J_m \dot{\omega} + B_m \omega} \tag{4}$$

The total efficiency of the motor is obtained as

$$\eta = \eta_{m1} * \eta_{m2} \tag{5}$$

### 2) PUMP

The efficiency of the pump is mainly considered from the two aspects of volumetric efficiency and mechanical efficiency. Volumetric efficiency is related to the compressibility of hydraulic oil and pump leakage, and mechanical efficiency is related to mechanical losses caused by friction and the like.

For plunger pumps, leaks often occur between the cylinder and the flow plate or the shaft, and between the plunger and the cylinder bore. From the theory of hydraulic fluid mechanics, the leakage flow of the plunger pump can be expressed for:

$$\triangle \, Q_{pl} = \frac{C_{vp} D_p p_L}{2\pi \, \mu_c} \tag{6}$$

where, $\Delta Q_{pl}$ is the leakage flow, $C_{vp}$ is the hydraulic oil laminar leakage coefficient, $D_p$ is the theoretical displacement of the pump (m3/rad), and $\mu_c$ is the comprehensive dynamic viscosity of the hydraulic oil related to the system pressure and temperature of which expression is

$$\mu_c = \mu \exp\left[\alpha p_s - \beta \left(G_p - G_{p0}\right)\right] \tag{7}$$

where, $\alpha$ and $\beta$ are coefficients related to pressure and temperature, $\mu$ is dynamic viscosity of oil, $p_s$ is system pressure, $G_{p0}$ and $G_p$ are initial temperature and working temperature of plunger pump, respectively, and the temperature rise of the pump is $G_p = G_p - G_{p0}$. In addition, the thermal expansion of the hydraulic oil will also cause a large change in the bulk elastic modulus of the hydraulic fluid and the system flow rate. Therefore, the volumetric efficiency of the plunger pump is

$$\begin{aligned}\eta_{pv} &= 1 - \frac{\Delta Q_{pl}}{Q_p} = 1 - \frac{\Delta Q_{pl}}{D_p \omega_m} \\ &= 1 - \frac{C_{vp} p_L}{2\pi \, \mu_c \omega_m} \left(1 + \lambda \Delta G_p\right)\end{aligned} \tag{8}$$

where, $\lambda$ is the thermal expansion coefficient of the hydraulic oil, and $Q_p$ is the theoretical output flow of the pump.

### 3) HYDRAULIC VALVES

PFV is the main energy loss part of all hydraulic valves in the system with loss of throttling. the oil will also flow through the spool valve opening, which is approximately the orifice, and its flow rate equation is shown as

$$Q = CA\sqrt{\frac{2\Delta P}{\rho}} \tag{9}$$

Then the PFV total flow satisfies below:

$$Q = Cx\sqrt{\frac{2\Delta P_1}{\rho}} + \frac{\pi C d^2}{4}\sqrt{\frac{2\Delta P_2}{\rho}} + Cx\sqrt{\frac{2\Delta P_3}{\rho}} \tag{10}$$

In the working state, the PFV always has flow loss. In order to obtain the flow calculation formula, the pressure and flow relationship of the PFV under different input pressures is simulated and analyzed, and the result is shown in Fig 4.

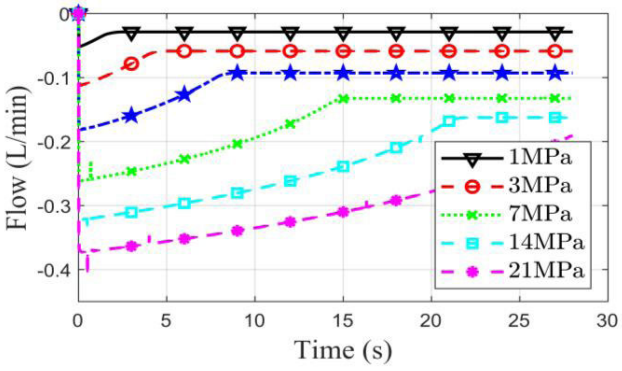


**FIGURE 4.** Leakage flow Curve of the PFV.

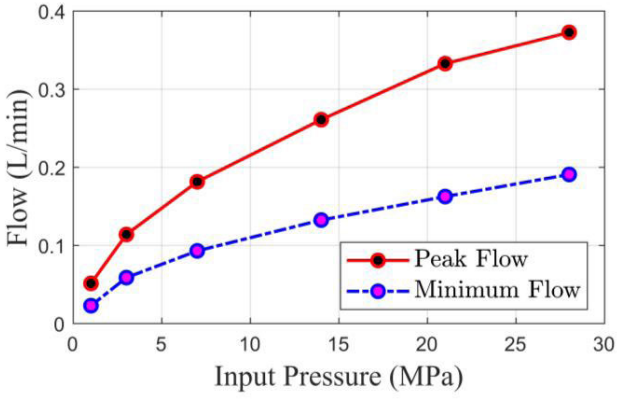


**FIGURE 5.** Pressure to flow curve of the PFV.

The leakage flow curve can be used to obtain the leakage flow of the PFV under different loads and output pressures. The leakage flow and the output pressure initially show a linear relationship. When the output pressure is equal to the input pressure, the leakage flow reaches a stable value.

The pressure to flow curve obtained from the above data is shown in Fig 5.

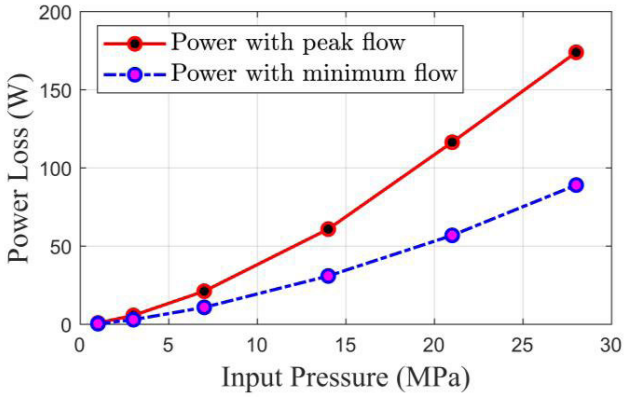


**FIGURE 6.** power loss curve of PFV.

Furthermore, the actual power loss curve of the PFV can be calculated as shown in Fig 6.

According to the simulation curves of Fig 5 and Fig 6, the leakage flow formula of the PFV can be fitted.

$$\Delta Q_v = 1.39 * 10^{-13} * P + 2.3 * 10^{-6} \tag{11}$$

*Remark:* In order to simplify the system model, the power loss of the pressure follower valve can be included in the loss of the actuator, and it can be expressed in the form of volumetric efficiency.

#### 4) ACTUATOR

Actuator efficiency also includes volume efficiency and mechanical efficiency. As mentioned in the previous section, in order to simplify the calculation, the PFV loss is approximately considered as the internal leakage of the actuator. From this, the volumetric efficiency expression of the actuator can be obtained

$$\eta_{cv} = 1 - \frac{\Delta Q_{cl} + \Delta Q_v}{Q_c} = 1 - \frac{C_{cl} p_L + C_{vl} p_L + \Delta Q_v}{\omega_m D_p} \tag{12}$$

where, $\Delta Q_{cl}$ and $\Delta Q_c$ are the leakage flow of the actuator and the total flow into the actuator, respectively, $C_{cl}$ and $C_{vl}$ are leakage coefficients. $\Delta Q_v$ meets the formula (11).

The mechanical loss of the actuator is also caused by friction, and its mechanical efficiency is expressed as:

$$\eta_{cm} = 1 - \frac{\Delta W_f}{W_f} = 1 - \frac{F_f x_c}{p_L A_c x_c} = 1 - \frac{F_f}{F_L} \tag{13}$$

where, $W_f$ is the total work done when the piston moves $x_c$, and $F_f$ is the friction between the piston of the actuator and the inner wall. Therefore, the total efficiency of the actuator is attained as:

$$\eta_c = \eta_{cv}\eta_{cm} = \left(1 - \frac{C_{cl} p_L + \Delta Q_v}{\omega_m D_p \eta_{pv}}\right)\left(1 - \frac{F_f}{F_L}\right) \tag{14}$$

#### 5) TOTAL SYSTEM EFFICIENCY

In summary, the total efficiency expression of the ALS-EHA is drawn below

$$\eta = \eta_{\mathrm{m}}\eta_{\mathrm{p}}\eta_{\mathrm{c}} = f\left(D_p, P_S, v, \dot{\omega}, \omega\right) \tag{15}$$

where, $D_p$ is the pump displacement, $P_S$ is the load pressure, $v$ is the moving speed of the actuator, and $\dot{\omega}$ is the angular acceleration of the motor.

If the motion speed, load pressure, and angular acceleration of the motor are taken as constant values and combined with the flow rate formula, the total efficiency of the system can be expressed as a single variable with displacement.

Given the actuator speed of 0.01m/s, the scatter plots of the total efficiency of the EHA system under load pressures of 7Mpa, 14Mpa, 21Mpa, and 28Mpa are drawn, as shown in Fig 7.

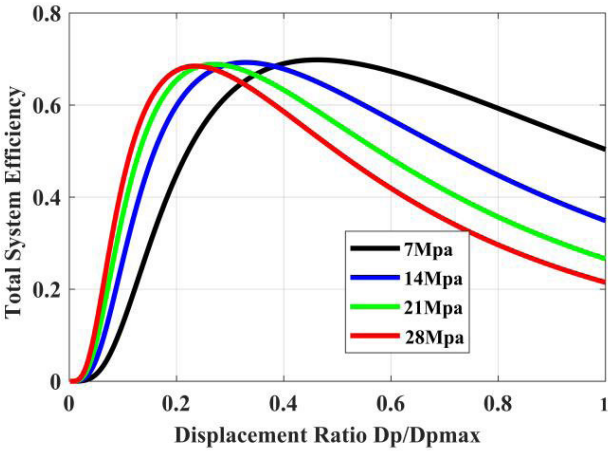


**FIGURE 7.** The curve of EHA efficiency to displacement ratio at v = 0.01.

It can be known from the observation curve that under this condition, the total system efficiency increases first and then decreases as the pump displacement ratio increases. This is because when the pump displacement is large, the system main loss is the copper loss of the motor, which can be effectively reduced through appropriately lowering the pump displacement ratio. When the pump displacement ratio is very small, further reducing the displacement ratio will decrease the overall system efficiency. This is because at this stage, the iron loss of the motor and the mechanical loss of the motor-pump set are the main loss, which especially the inertia moment loss accounts for the main proportion. Therefore, under certain working conditions, an optimal displacement value can make the system optimal efficiency. When the load pressure is 7MPa and the speed of the actuator is 0.01m/s, by designing a reasonable control law, the efficiency can be improved by up to 200%. The greater the system load pressure, the more obvious the system efficiency improves.

Increasing the motor-pump set speed, given the actuator speed of 0.05m/s, the scatter diagram of the total efficiency of the EHA system is drawn under load pressures of 7Mpa, 14Mpa, 21Mpa, and 28Mpa, as shown in Fig 8.

Observing the above figure, it can be found that the system efficiency with the change of the displacement ratio still mainly presents a trend of first increase and then decrease. However, comparing and analyzing Fig 7 and Fig 8, it can be observed that the system efficiency curve shifts obviously

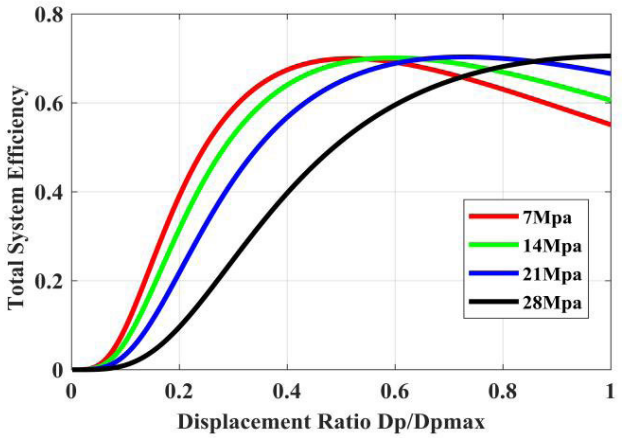


**FIGURE 8.** The curve of EHA efficiency to displacement ratio at v = 0.05.

to the right when the speed is increased compared with the operating speed of 0.01m/s. When the load is 7MPa, the system decline trend is not obvious. This is because the speed of the motor-pump set is significantly higher than that at the previous condition under this condition, and the proportion of motor iron loss and pump efficiency loss is significantly larger than that at low speed. Therefore, under this condition, the optimal efficiency point corresponds to an increase in the optimal displacement value.

However, it should be noted that the total system efficiency and the motor heating are not exactly the same concept. In other words, when the total system efficiency is the highest, the motor heat output is not necessarily the minimum point. This is because the volume and mechanical loss of the pump also cause power loss. Therefore, when designing the control law, it is necessary to determine whether it is necessary to maximize system efficiency or minimize motor heating. Of course, the gap between the two may not be obvious. This paper mainly considers the situation with the highest system efficiency.

### B. IV. DYNAMIC ANALYSIS OF ALS

To simplify the system model, it is now assumed that the external load force is an elastic load, that is $F_L = Kx$, assuming the system is initially in a zero state. Then combining the flow equations of the pump and actuator, with the dynamic equation of the actuator, we can get the following relationship.

$$(D_p - C_n)\omega = a_1 x + a_2 \ddot{x} + a_3 \dot{x} + a_4 x \tag{16}$$

where

$$a_1 = \frac{Vm_a}{\beta A_a}, a_2 = \frac{VB_a + (C_a + C_p)\beta m_a}{\beta A_a}$$
$$a_3 = \frac{A_a^2 + VK + (C_a + C_p)\beta B_a}{\beta A_a}, a_4 = \frac{(C_a + C_p)K}{A_a}$$

The Laplace transform of the above formula can get the hydraulic part transfer function of the system.

$$\frac{x(s)}{\omega(s)} = \frac{(D_p - C_n)}{a_1 s^3 + a_2 s^2 + a_3 s + a_4 K} \tag{17}$$

According to the above formula, in the hydraulic part transfer function, the displacement of the pump is located in the numerator of the transfer function. If the denominator of the system is unchanged, the larger the displacement value, the larger the numerator. So the following conclusion can be obtained: under the premise of stable system, for the hydraulic part of the EHA system, the larger the displacement of the variable pump, the faster the system's dynamic response.

In the same way, combined with the motor mathematical model, the below equation can be obtained

$$U = \frac{LJ}{K_t}\ddot{\omega} + \frac{JR + LB}{K_t}\dot{\omega} + \frac{BR + K_e K_t}{K_t}\omega + \frac{LD_p m_a}{K_t A_a}x + \frac{B_a L D_p + m_a D_p R}{K_t A_a}\ddot{x} + \frac{LKD_p + B_a D_p R}{K_t A_a}\dot{x} + \frac{KD_p R}{K_t A_a}x \tag{18}$$

Laplacian transform to the above formula, it can be obtained

$$U(s) = G_1(s)\,\omega(s) + G_2(s)\,x(s) \tag{19}$$

where

$$G_1(s) = \frac{LJs^2 + (JR + LB)s + BR + K_e K_t}{K_t}$$
$$G_2(s) = D_p \frac{Lm_a s^3 + (B_a L + m_a R)s^2 + (LK + B_a R)s + KR}{K_t A_a}$$

Bringing the hydraulic part transfer function of the system into the above formula, the following equation can be obtained

$$U(s) = G_1(s)\frac{f(s)}{(D_p - C_n)}x(s) + G_2(s)\,x(s) \tag{20}$$

where

$$f(s) = a_1 s^3 + a_2 s^2 + a_3 s + a_4 K$$

We observe the above formula (20) in combination with actual system parameters, the order of magnitude for the 0th order coefficient of the second term on the right reaches $10^6$ and that for the first term is 1-10. Therefore, the first term on the right has a greater impact on the dynamic speed adjustment of the system. Ignoring the second item on the right, the below equation can be gotten

$$\frac{x(s)}{U(s)} = \frac{(D_p - C_n)}{f(s)\,G_1(s)} \tag{21}$$

Then in the expression of the system output $x$ to system input U, the system displacement is only in the numerator part. Given the system denominator is unchanged, the larger the displacement is, the larger the numerator is. Therefore, under the current assumptions, we can draw the following conclusions: For ALS-EHA system, because the variation in

pump displacement does not change the moment of inertia, under the premise of constant input. The larger the system displacement is, the faster the speed adjustment is, and the better the dynamic performance of the system is.

## IV. CONTROL ALGORITHM

In order to solve the contradiction between high dynamics and high efficiency of the EHA system, we need to make the motor and the entire EHA system work as high efficiently as possible, but still increase the displacement ratio as much large as possible to improve the system Dynamic performance.

However, considering the characteristics of the ALS-EHA system, that is, the displacement adjustment range of the pump is actually closely related to the operating conditions (hydraulic system load pressure), which results in the system output being a non-linear function of displacement; Meanwhile, the definition range of displacement also varies with the working conditions; combining with the multiplied nonlinearity between the motor speed and the pump displacement, the overall nonlinearity of the system is extremely strong. Therefore, combined with the previous analysis, this paper proposes an energy optimal control law based on fuzzy and disturbance compensation.

### A. EFFICIENCY OPTIMIZING

Different from the conventional EHA system with variable-speed variable-displacement, since the ALS-EHA system introduces the system high-pressure cavity pressure into a PFV and relies on the control of the PFV opening to actively control the pump displacement, therefore, the active load is sensitive. The pump displacement adjustment range for the ALS-EHA system is closely related to the load pressure, as shown in Fig 9.

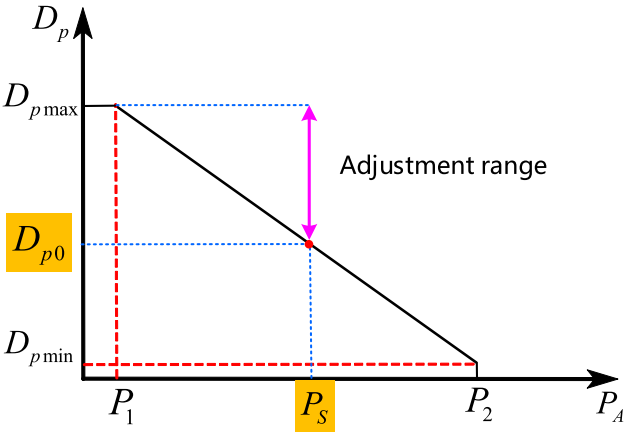


**FIGURE 9.** Load-sensitive pump displacement adjustment curve.

It can be expressed as:

$$D_p = g(P_A) = \begin{cases} D_{p\max}\left[1 - \frac{A_v}{K_S x_{v0}}(P_A - P_1)\right] & (P_1 < P_A < P_2) \\ D_{p\max} & (P_A \le P_1) \end{cases} \tag{22}$$

In the formula: $D_{p\max}$ is the maximum displacement of the load-sensitive pump, and is also the initial displacement; $A_v$ is the effective area of the variable mechanism; $K_S$ is the stiffness of the back pressure spring (N/mm); $x_{v0}$ is the displacement of the variable mechanism at load pressure 0, and is also the initial displacement (mm); $P_1$ is the pre-compression pressure of the back pressure spring.

Since the input pressure of the variable pump comes from the output pressure of the PFV, by controlling the PFV opening, the input pressure of the swash plate variable mechanism can be controlled from 0 to $P_S$. According to the displacement adjustment characteristics, the displacement ratio $\beta$ can range from 0 to 1.

First, the real-time position signal of the system and the pressure signal of the shuttle valve outlet (that is, the pressure of the high-pressure chamber of the EHA system) are sampled. Therefore, the current real-time speed of the ALS-EHA system can be obtained. Ignoring the leak, the relationship is derived from the flow conservation equation:

$$\omega = \frac{A_a \dot{x}}{D} \tag{23}$$

That is, in actual working conditions, the motor speed can be expressed by the speed of the actuator and the displacement of the pump. Where the moving speed of the actuator is a measurable variable (derived from the position derivative). The above equation is brought into the efficiency equation of the ALS-EHA system, the efficiency function $\eta = f(D)$ for displacement D is obtained. In each cycle, by solving the maximum value of the efficiency function within the constraint range, the pump displacement corresponding to the highest point of system efficiency can be obtained, defining the displacement $D_p^*$ at this time. The ALS-EHA system's decisions between high efficiency and high dynamics can be attained by adjusting the pump displacement ratio at $\left(D_p^*, D_{p\_\max}\right)$.

Since the pump's displacement adjustment range is related to the system's real-time working load pressure. As mentioned earlier, when the input pressure of the variable pump swashplate is $P_S$, the corresponding displacement is $D_{p0}$. The calculation method can be obtained from the previous paragraph. The maximum displacement adjustment range of the pump is $\left(D_{p0}, D_{p\_\max}\right)$. Because the relative size relationship between $D_{p0}$ and $D_p^*$ varies with the system power, the concept of effective displacement adjustment range is defined here, which represents the range of displacement that can be effectively adjusted in the actual operating conditions to effectively adjust the system efficiency. The actual corresponding effective displacement adjustment range is $\left(\max\left(D_p^*, D_{p0}\right), D_{p\_\max}\right)$, as shown in Fig 10.

In actual working conditions, generally within the effective adjustment range, the system efficiency shows a decreasing relationship. When the optimal displacement ratio of the current working condition is determined, the corresponding PFV output pressure can be obtained. According to the PFV model, the actual control current of the PFV can be obtained.

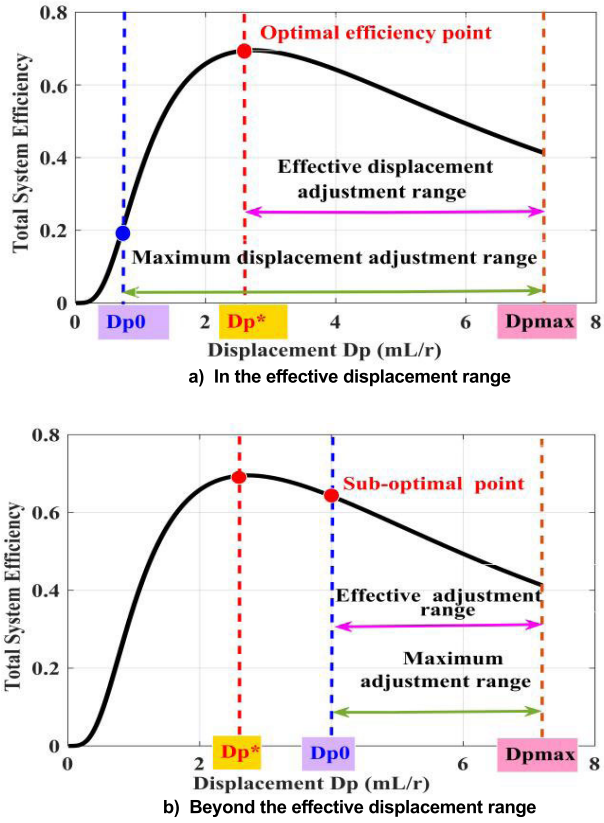


**FIGURE 10.** Schematic diagram of adjustment range of displacement.

The variable pump displacement matching the system's optimal efficiency point is solved below.

According to formula (15) $\eta = \eta_m\eta_p\eta_c = f\left(D_p, P_S, v, \dot{\omega}\right)$, in the actual system, the load pressure $P_S$, the speed of the actuator $v$ and the angular acceleration of the motor $\dot{\omega}$ can be measured, then the overall efficiency $\eta$ and the pump displacement $D_p$ satisfy

$$\eta = f\left(D_p\right)\Big|_{P_S,v,\dot{\omega}} \tag{24}$$

**TABLE 2.** Fuzzy rule.

| Ec \ E | NB | NM | NS | 0 | PS | PM | PB |
|---|---|---|---|---|---|---|---|
| NB | PVB | PVB | PVB | PB | PRS | 0 | 0 |
| NM | PVB | PB | PRB | PM | PRS | 0 | 0 |
| NS | PRB | PM | PRS | PS | 0 | 0 | 0 |
| 0 | PM | PRS | 0 | 0 | 0 | PRS | PM |
| PS | 0 | 0 | 0 | PS | PRS | PM | PRB |
| PM | 0 | 0 | PRS | PM | PRB | PB | PVB |
| PB | 0 | 0 | PRS | PB | PVB | PVB | PVB |

Let $D_p^*$ be the displacement corresponding to the highest point of system efficiency, then

$$D_p^* = f^{-1}\left(\eta^*\right)\Big|_{\eta^*=\max(\eta)} \tag{25}$$

According to formula (24), we can get

$$P_A^* = g^{-1}(D_p^*) = g^{-1}(f^{-1}\left(\eta^*\right)\Big|_{\eta^*=\max(\eta)}) \tag{26}$$

where, $P_A^*$ is the PFV output pressure needed to meet displacement corresponding to the optimal efficiency of the system.

Due to the characteristics of the ALS-EHA system, the maximum adjustment range of the pump's displacement will varies with the change of the system load pressure. Now $D_{p0}$ is defined as the corresponding value when the output pressure of the PFV is equal to the system load pressure $P_S$. Then the actual maximum displacement range of the system is $\left[D_{p0}, D_{p\max}\right]$. Combined with the optimal point of ideal efficiency, the displacement adjustment range is $\left[\max(D_p^*, D_{p0}), D_{p\max}\right]$.

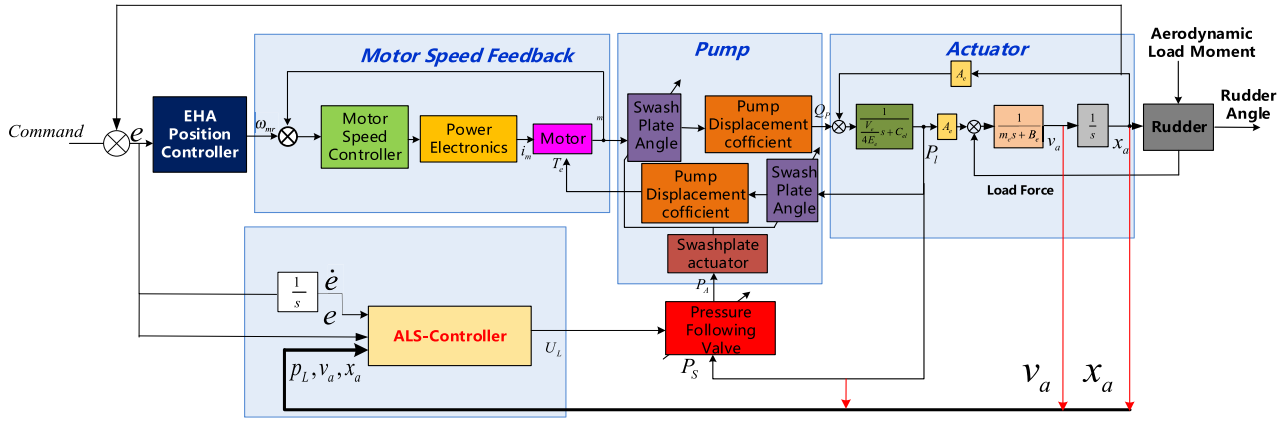


**FIGURE 11.** The schematic for ALS-EHA control system.

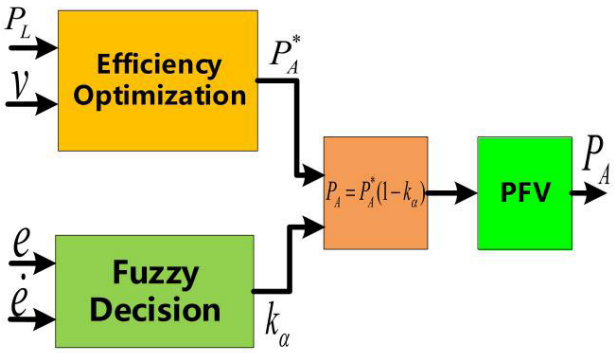


**FIGURE 12.** Control block diagram.

We Modify equation (28), the optimal efficiency control law can be obtained

$$P_A^* = g^{-1}(\max(D_p^*, D_{p0})) = g^{-1}(\max(f^{-1}(\eta^*)\big|_{\eta^*=\max(\eta)}, D_{p0})) \quad (27)$$

### B. DYNAMIC CONSTRAINT BASED ON FUZZY RULES

In order to ensure the dynamic performance of the system, it is necessary to determine the real-time operating conditions of the system to ensure that the system can meet the needs of servo tracking. Because the dynamic performance of the system is directly related to the displacement of the pump, a multi-loop PID is used to control the motor pump main loop, and a fuzzy controller is used to control the displacement of the pump. The control schematic is shown in the Fig 11.

In order to accurately represent the dynamic performance of the system, while considering the current state and predicting the state of the future moment, the position error and the position error differential of the system are required as fuzzy inputs for judgment. When the dynamic performance of the system is poor, the displacement of the variable pump needs to be appropriately increased; when the system tracking performance is good, the displacement of the variable pump can be maintained or appropriately reduced. According to the above rules, the fuzzy rules of the system are shown in the table 2.

Its input is the system's position error and position error derivative (that is, speed error), the fuzzy subset is {NB, NM,

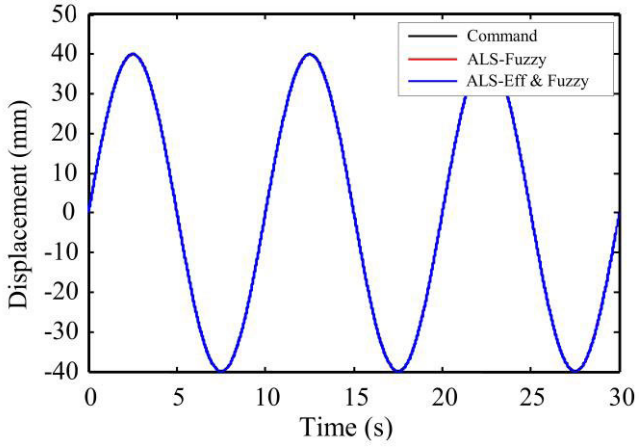


a) Position response curve

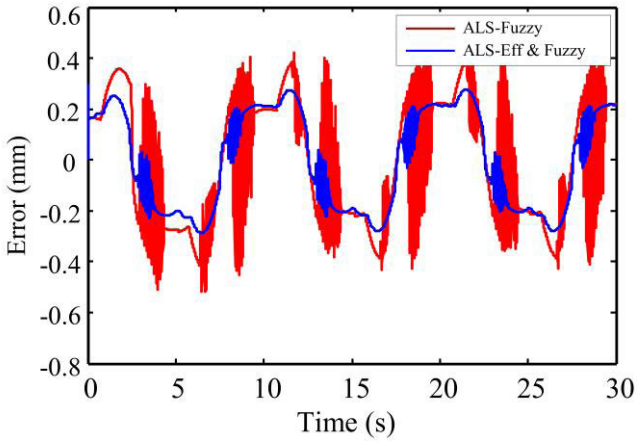


b) Position error curve

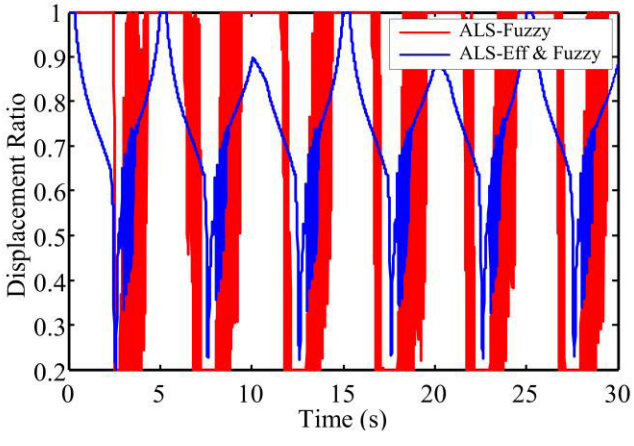


c) Displacement ratio change curve

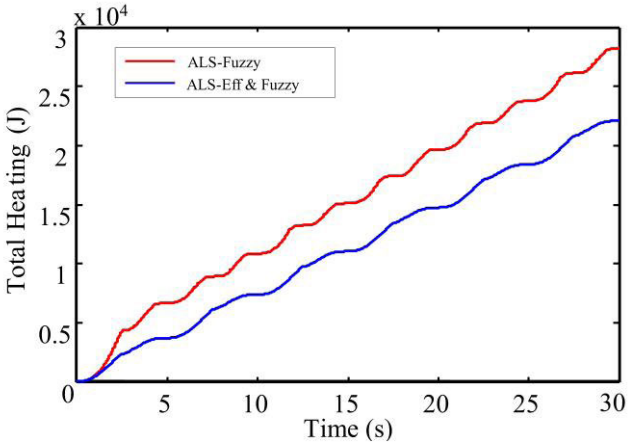


d) Motor heating curve

**FIGURE 13.** Low-speed large-load simulation curve.

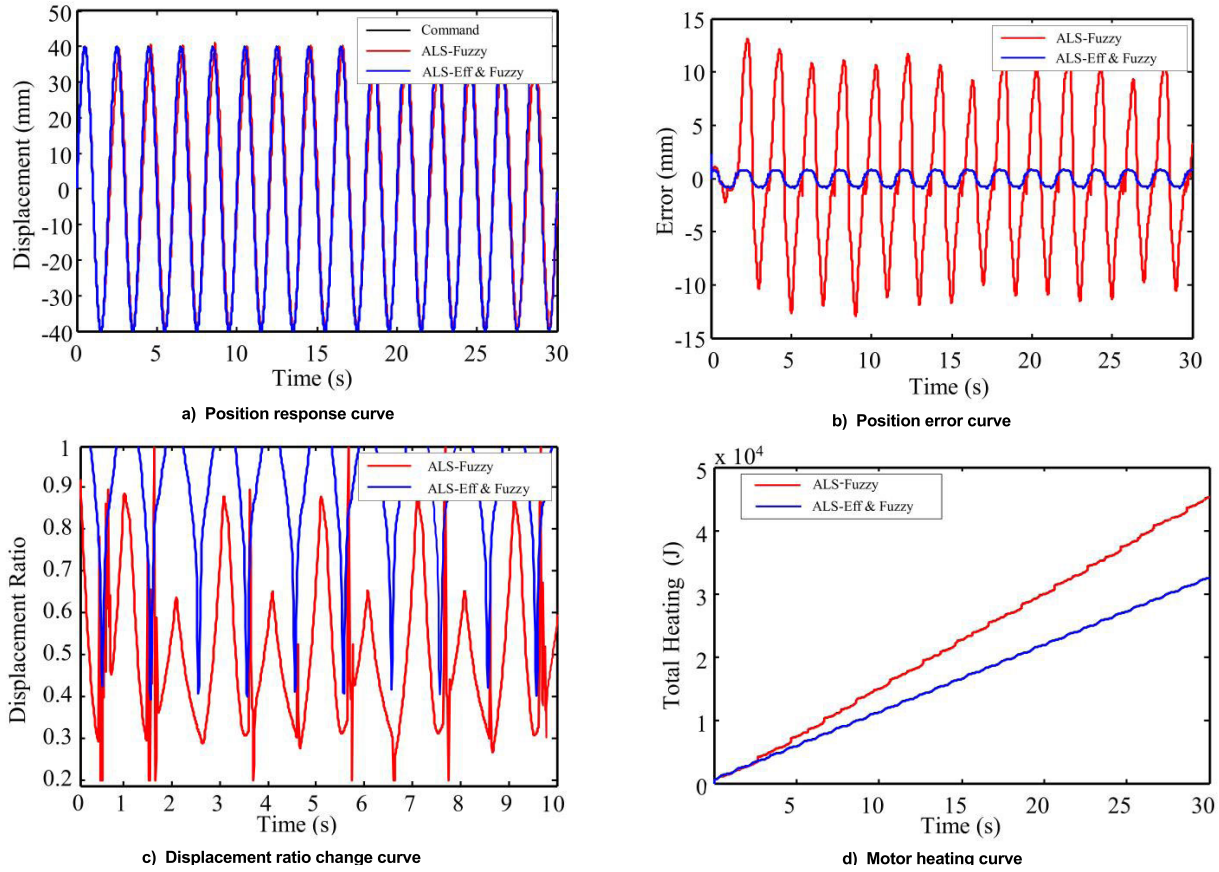


**FIGURE 14.** High-speed large-load simulation curve.

NS, 0, PS, PM, PB}, and the output is the dynamic adjustment coefficient, which is defined here as $k_\alpha$. The fuzzy subset is {0, PS, PRS, PM, PRB, PB, PVB}, and the variation range is between 0-1. The larger the value, the higher the output pressure of the PFV, that is, the larger the displacement ratio of the variable pump.

The fuzzy rules described in table 2 will give a more reasonable description of the tracking performance of the system, that is, the worse the dynamic performance of the system, the larger the displacement ratio obtained by the fuzzy rules, thereby improving the dynamic performance of the system; The dynamic performance of the system is better, the displacement ratio of the variable pump is maintained or appropriately reduced. This is consistent with previous principles of judgment.

The output pressure of the PFV is corrected according to the fuzzy rule. The corrected output pressure is drawn below

$$P_A = P_A^*(1 - k_\alpha) = P_A^*(1 - k_\alpha) \tag{28}$$

### C. LOAD DISTURBANCE COMPENSATION

The output pressure of the PFV is not only related to its control current, but also to the load pressure of the system. When the external load force is disturbed, the PFV output will also fluctuate accordingly, which will cause the displacement of the variable pump to fluctuate, affecting the stability of the system.

In order to improve the disturbance rejection ability of the system, an additional load disturbance compensation $\Delta P_A$ is defined here to satisfy $\Delta P_A = k \cdot \Delta P_S$. Where $\Delta P_S$ is the system pressure disturbance. When $\Delta P_S$ is positive, the pressure disturbance forces the displacement to decrease. At this time, $P_A$ needs to be reduced to compensate for the effect of the disturbance on the pump displacement ratio. When $\Delta P_S$ is negative, the pressure disturbance increases the displacement, then it need to increase $P_A$ to compensate the effect of disturbance on the pump displacement ratio.

Combining the above points, it can conclude that the actual output pressure of the PFV is:

$$P'_A = P_A^*(1 - k_\alpha) - \Delta P'_A = P_A^*(1 - k_\alpha) - k \cdot \Delta P_S \tag{29}$$

where, $P_A^*$ is the output pressure value of the PFV corresponding to $\max\left(D_p^*, D_{p0}\right)$. $P'_A$ is the output pressure after comprehensively considering the optimal efficiency, dynamic constraints and load disturbance, and $k$ is the load Perturbation compensation coefficient.

### D. CONTROL LAW DESIGN

Combining the above sections, it can obtain the optimal energy control law based on fuzzy and disturbance compensa-

tion. According to the formulas (27), (28) and (29), the actual input current of the PFV can be obtained. That is, for the load-sensitive loop, the control input is

$$u = \frac{P_S - (1-k_\alpha)\cdot g^{-1}(\max(f^{-1}(\eta^*)\big|_{\eta^*=\max(\eta)}, D_{p0}) - k\Delta P_S}{K_A} \tag{30}$$

According to the designed control law, the control block diagram of the system is shown in Figure 38.

## V. SIMULATION AND EXPERIMENTAL ANALYSIS

### A. COMPARATIVE ANALYSIS

In order to verify the performance of the ALS-EHA system with the based fuzzy and disturbance compensation energy optimal control law, the control law is compared with the traditional fuzzy control law. The control law described in [28] is: the motor loop adopts multi-loop PID control, the load sensitive loop only uses fuzzy control, the fuzzy input is position error and system load pressure, and the fuzzy output is the ratio of the outlet pressure of the PFV to the inlet pressure.

In the following simulation curves, ALS-Fuzzy is used to represent the control law using only fuzzy control, and ALS-Eff & Fuzzy is used to represent the energy optimal control law proposed based on fuzzy and disturbance compensation in this paper.

#### 1) LOW SPEED AND HEAVY LOAD

The position command signal is a sinusoidal signal with a frequency of 0.1 Hz and an amplitude of 40 mm, and the load is a spring load with a stiffness $3.5*10^6$ N/m and a damping 1000 N/(m/s) The simulation results are shown in Fig 13.

It can be seen from the simulation results that under low-speed and large-load conditions, the tracking performance of the two is similar. In terms of motor heating, ALS-Eff & Fuzzy generates less heat.

#### 2) HIGH-SPEED AND HEAVY-LOAD

The given position command signal is a sinusoidal signal with a frequency of 0.5 Hz and an amplitude of 40 mm, and the load is a spring with stiffness $3.5*10^6$N/m and damping 1000 N/(m/s). The simulation curve is shown in Fig 14.

Observing the curve, we can find that under high-speed and heavy-load operating conditions, the ALS-Eff & Fuzzy has good tracking performance, while the ALS-Fuzzy has poor tracking performance, of which tracking error exceeds 10mm. In terms of motor heating, the ALS-Eff & Fuzzy generates less heat, and the pump displacement ratio is higher, indicating that the control law has successfully found the optimal point of efficiency with disturbance compensation. Under high-speed and heavy-load conditions, the performance of the ALS-Eff & Fuzzy is better.

#### 3) DYNAMIC PERFORMANCE TEST

To verify the tracking performance of the system under heavy load conditions, given the external load force of the system

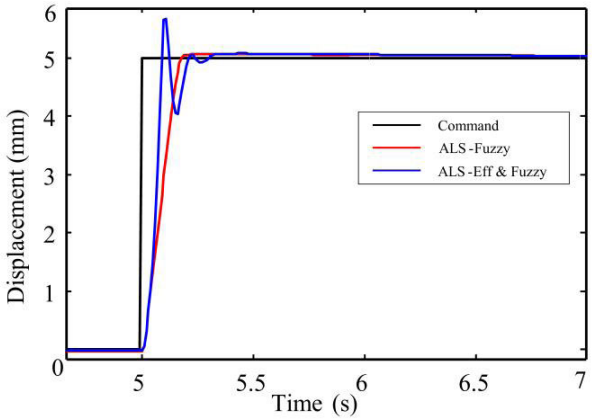


a) Position response curve

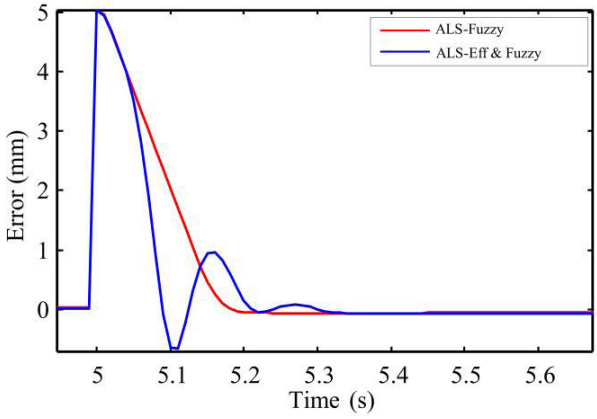


b) Position error curve

**FIGURE 15.** Step response test.

to 180000N (close to full load), the initial position is 0, and a 5mm step signal is given at 1s.

It can be known from the position response curve and the position error curve that under this condition, the rise time of ALS-Fuzzy is about 200ms, and the rise time of ALS-Eff & Fuzzy is about 100ms, which is much shorter than the time required by ALS-Fuzzy. The settleing time of the former is much faster than that of the latter, its overshoot a little higher.but It can be seen that the dynamic performance of the ALS-Eff & Fuzzy is better.

Combining all the simulation results in this section, the following conclusions can be drawn: The ALS-Eff & Fuzzy has better both dynamic performance and efficiency performance under the heavy load condition.

#### 4) TYPICAL LOAD SPECTRUM

In order to verify the performance of the system and the control law in actual flight, a simulated flight curve is given for comparative simulation analysis. The load is a spring load with a stiffness and a damping of 1000. The obtained system simulation curves are shown in Fig 16.

Fig 16 shows the position response and position error curves of the system. It can be found that under typical load spectrum conditions, the tracking error tracking accuracy of

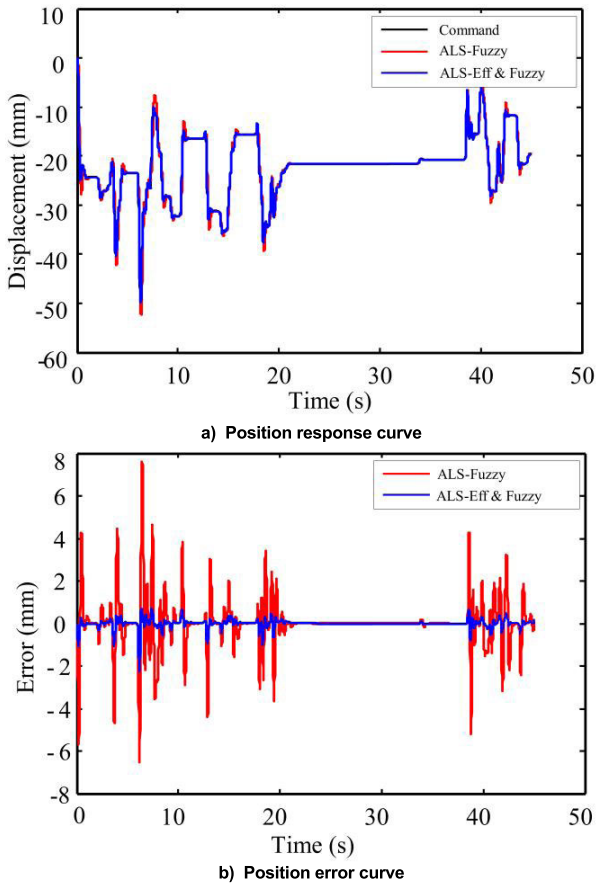


**FIGURE 16.** Position response and error curve.

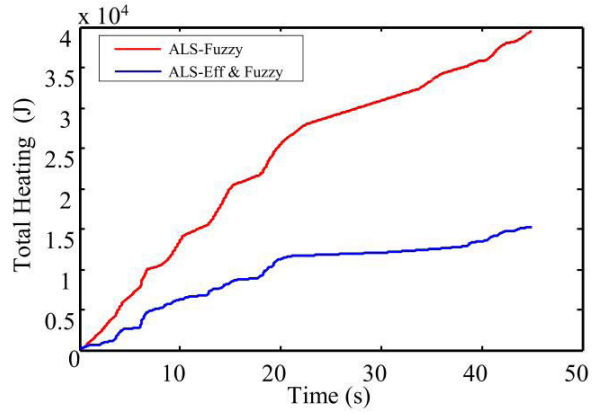


**FIGURE 17.** Motor heating curve.

the ALS-Eff & Fuzzy is higher. When the position command fluctuates greatly, the position output error through the control law designed in this paper is smaller and the disturbance rejection ability is stronger.

Fig 17 shows the heating curve of the motor under this condition. It can be found that the motor of the ALS-Eff & Fuzzy generates less heat. Combining the above two points, it can be known that the ALS-Eff & Fuzzy has better performance.

## VI. CONCLUSION

Based on the above results, several advantages of ALS-EHA with the energy optimal control law based on fuzzy and disturbance compensation designed in this paper can be summarized:

1) The system efficiency is optimized in real time to ensure that the system operates in the high efficiency range;

2) Combined with fuzzy control, real-time adjustment of displacement according to working conditions, the system dynamic performance is better;

3) Introduce load disturbance compensation to avoid displacement instability caused by load disturbance, and the system has strong disturbance rejection ability;

4) For Low-speed operation, small displacement is usually used to increase the speed of the motor-pump set, avoiding the low-speed unstable region of the motor-pump set, so the system has better control performance and more stable low-speed operation.

In addition, the idea of efficiency matching is also applicable to the design of the parameters of the FPVM-EHA system. As long as the common load spectrum of the aircraft is given and the long-term operating point of the system is determined, a relatively optimal displacement value can be reasonably designed based on the idea of efficiency matching.

Of course, this result requires repeated iterative design, because for a pump, its displacement will affect its rotational inertia. When designing the motor, the rotational inertia of the pump is a influence factor that cannot be ignored, which has a great influence on the power curve of the motor; and the power curve of the motor will in turn affect the rotational inertia of the motor and the relevant parameters of the pump. The entire design process is coupled. Repeated iterative design is required to determine the parameter index of each part of the system. Although the process is complicated, according to the previous analysis, it can be considered that the efficiency matching design is able to increase the overall efficiency performance of the system, which is of great significance for the wide application of EHA systems.

## REFERENCES

[1] G.-H. Jung, "Start and stop characteristics of single-rod electro-hydrostatic actuator," *Trans. Korean Soc. Mech. Eng.*, vol. 35, no. 11, pp. 1483–1490, Nov. 2011, doi: 10.3795/KSME-A.2011.35.11.1483.

[2] X. Y. Qi, "Research on the principle of airborne power transmission actuator," Ph.D. dissertation, Dept. Mech. Eng., BH. Univ., Beijing, China, 2001.

[3] Y. Luo, "Development trend of airborne integrated actuation system," *Chin. Hydraul. Pneum.*, no. 1, pp. 1–3, 2004, doi: 10.3969/j.issn.1001-3881.2004.01.001.

[4] H. S. Ling, "The prototype of next-generation aircraft steering gear-F/A-18 smart aileron steering gear," *Int. Aviat.*, vol. 3, pp. 53–54, Dec. 1993.

[5] J. Long, "Development trend of new aircraft actuation system," *Aeronaut. Sci. Technol.*, vol. 1, pp. 11–13, Oct. 2000.

[6] X. Y. Qi, Y. L. Fu, and Z. L. Wang, "Analysis of power teleport airborne actuation system scheme," *J. BH Univ. Aeronaut.*, vol. 25, no. 4, pp. 426–430, 1999.

[7] S. L. Botten, C. R. Whitley, and A. D. King, "Flight control actuation technology for next-generation all-electric aircraft," *Technol. Rev. J.*, vol. 8, pp. 55–68, Oct. 2000.

[8] J. A. Anderson, "Variable displacement electro-hydrostatic actuator," in *Proc. IEEE-NAECON*, Dayton, OH, USA, 1991, pp. 529–534, doi: 10.1109/NAECON.1991.165801.

[9] S. Habibi, J. Roach, and G. Luecke, "Inner-loop control for electromechanical (EMA) flight surface actuation systems," *J. Dyn. Syst., Meas., Control*, vol. 130, no. 5, pp. 1002–1013, Sep. 2008, doi: 10.1115/1.2936382.

[10] S. Habibi and A. Goldenberg, "Design of a new high-performance electrohydraulic actuator," *IEEE/ASME Trans. Mechatronics*, vol. 5, no. 2, pp. 158–164, Jun. 2000, doi: 10.1109/3516.847089.

[11] S. Li, Y. Shang, S. Wu, Y. Zhou, and Z. Jiao, "Investigation the load matching of direct pressure valve controlled variable mechanism of axial variable piston pump," in *Proc. IEEE Int. Conf. Cybern. Intell. Syst. (CIS) IEEE Conf. Robot., Autom. Mechatronics (RAM)*, Nov. 2017, pp. 434–438, doi: 10.1109/ICCIS.2017.8274815.

[12] J.-H. Kim, C.-S. Jeon, and Y.-S. Hong, "Constant pressure control of a swash plate type axial piston pump by varying both volumetric displacement and shaft speed," *Int. J. Precis. Eng. Manuf.*, vol. 16, no. 11, pp. 2395–2401, Oct. 2015, doi: 10.1007/s12541-015-0309-5.

[13] B. Gao, Y. L. Fu, Z. C. Pei, and J. M. Ma, "Research on dual-variable integrated electro-hydrostatic actuator," *Chin. J. Aeronaut*, vol. 19, pp. 77–82, Dec. 2006, doi: 10.1016/S1000-9361(11)60271-9.

[14] Y. Zhang, Y. Fu, and W. Zhou, "Optimal control for EHA-VPVM system based on feedback linearization theory," in *Proc. 11th Int. Conf. Control Autom. Robot. Vis.*, Dec. 2010, pp. 744–749, doi: 10.1109/ICARCV.2010.5707815.

[15] Y. L. Fu, H. T. Qi, Y. L. Lu, R. S. Guo, Z. F. Li, J. Xue, and Q. Yang, "A novel electrical servo variable displacement hydraulic pump used for integrated actuator in MEA," in *28th Proc. ICAS*, Brisbane, Australia, Sep. 2012, pp. 23–28.

[16] S. D. Kim, H. S. Cho, and C. O. Lee, "A parameter sensitivity analysis for the dynamic model of a variable displacement axial piston pump," *Proc. Inst. Mech. Eng. Part C-J. Mech. Eng. Sci.*, 1987, pp. 235–243, doi: 10.1243./PIME_PROC_1987_201_115_02.

[17] Z. Li, Y. Shang, Z. Jiao, Y. Lin, S. Wu, and X. Li, "Analysis of the dynamic performance of an electro-hydrostatic actuator and improvement methods," *Chin. J. Aeronaut.*, vol. 31, no. 12, pp. 2312–2320, Dec. 2018, doi: 10.1016/j.cja.2018.03.014.

[18] W. Hu, L. Zhou, Y. Tian, Z. Jiao, Y. Shang, Z. Song, and L. Yan, "Analysis for the power loss of electro hydrostatic actuator and hydraulic actuator," in *Proc. IEEE Int. Conf. Adv. Intell. Mechatronics (AIM)*, Jul. 2015, pp. 613–616, doi: 10.1109/AIM.2015.7222604.

[19] J. Willkomm, M. Wahler, and J. Weber, "Potentials of speed and displacement variable pumps in hydraulic applications," in *Proc. IFPC*, Dresden, Germany, Mar. 2016, pp. 379–391.

[20] J. C. Mare, G. Vinson, T. Prado, and M. Combacau, "Modelling and simulating the pump of an aerospace electro-hydrostatic module for fault detection and identification purposes," in *Proc. ASME/BATH FPMC, BATH*. U.K.: ASME, Sep. 2014, Art. no. V001T01A002, doi: 10.1115/FPMC2014-7803.

[21] J.-Y. Oh, G.-H. Jung, G.-H. Lee, Y.-J. Park, and C.-S. Song, "Modeling and characteristics analysis of single-rod hydraulic system using electro-hydrostatic actuator," *Int. J. Precis. Eng. Manuf.*, vol. 13, no. 8, pp. 1445–1451, Aug. 2012, doi: 10.1007/s12541-012-0190-4.

[22] T. Sakuma, K. Tsuda, K. Umeda, S. Sakaino, and T. Tsuji, "Modeling and resonance suppression control for electro-hydrostatic actuator as a two-mass resonant system," *Adv. Robot.*, vol. 32, no. 1, pp. 1–11, Jan. 2018.

[23] J.-C. Maré and J. Fu, "Review on signal-by-wire and power-by-wire actuation for more electric aircraft," *Chin. J. Aeronaut.*, vol. 30, no. 3, pp. 857–870, Jun. 2017, doi: 10.1016/j.cja.2017.03.013.

[24] N. Alle, S. S. Hiremath, S. Makaram, K. Subramaniam, and A. Talukdar, "Review on electro hydrostatic actuator for flight control," *Int. J. Fluid Power*, vol. 17, no. 2, pp. 125–145, May 2016, doi: 10.1080/14399776.2016.1169743.

[25] A. Jafari, N. G. Tsagarakis, and D. G. Caldwell, "A novel intrinsically energy efficient actuator with adjustable stiffness (AwAS)," *IEEE/ASME Trans. Mechatronics*, vol. 18, no. 1, pp. 355–365, Feb. 2013, doi: 10.1109/TMECH.2011.2177098.

[26] Q. Chao, J. Zhang, B. Xu, Y. Shang, Z. Jiao, and Z. Li, "Load-sensing pump design to reduce heat generation of electro-hydrostatic actuator systems," *Energies*, vol. 11, no. 9, p. 2266, Aug. 2018, doi: 10.3390/en11092266.

[27] B. Johansson, J. Andersson, and P. Krus, "Thermal modeling of an electro-hydrostatic actuation system," in *Proc. RAAH*, Toulouse, France, 2001.

[28] Z. H. Li, "Research on Energy Matching and Performance Control of Airborne Power Transmission by Electro-Hydrostatic Actuation System," Ph.D. dissertation, Automat., Beihang Univ., Beijing, China, 2018.


**LIGANG HUANG** received the B.S. degree in electric engineering from Hebei Normal University, Shijiazhuang, China, in 2011, and the M.S. degree in control engineering from the Shenyang University of Technology, Shenyang, China, in 2015. He is currently pursuing the Ph.D. degree in mechatronic engineering with Beihang University, Beijing, China.

His main research interests are electro-hydraulic servo control including EHA and load simulator' control. His awards and honors include SMC Fellowship, President's scholarship of Beihang University.

**TIAN YU** (Member, IEEE) received the B.E. degree in mechanical engineering from Northwestern Polytechnical University, China, in 2012, the M.S. degree in fluid power engineering from the University of Bath, U.K., in 2013, and the Ph.D. degree from the University of Bath on actuation and control of lower limb prostheses, in 2017.

He is currently working as a Lecturer with Beihang University. From 2013 to 2017, he was a Research Assistant with the Fluid Dynamics and Laboratory, Bath University. He is current research interests include fluid transmission, electrohydrulic control and rehabilitation robots as well as EHA. His awards and honors include graduate scholarship (Bath University), best paper award, and Royal Designer for Industry.

**ZONGXIA JIAO** (Senior Member, IEEE) received the B.S. and Ph.D. degrees in mechatronics engineering from Zhejiang University, Hangzhou, China, in 1985 and 1991, respectively.

From 1991 to 1993, he was as a Postdoctoral Fellow with Beihang University, where he became a Professor, in 1994. In 2000, he was invited to the Institute for Aircraft System Engineering, Technische Universit&auml, TU Hamburg-Harburg, as a Visiting Professor. He is the Director of the National Defense Key Laboratory of Integrated Flight Control Technology, Beihang University. He is President of FPM and ICIEA international conference, in 2011 He is currently the Dean of the Ningbo Innovation Research Institute, Beihang University. His research interests include fluid power and transmission, actuators, and sensors. He has published more than 150 articles, and more than 70 articles have been included in SCI/EI/ISTP three retrieval systems. He has published and compiled eight books and won more than ten invention patents. He has won the second prize of national technology invention and the second prize of scientific and technological progress.

**YANPENG LI** received the B.S. and M.S. degrees in mechanical engineering from Yanshan University, Qinhuangdao, China, in 2013 and 2016, respectively. He is currently pursuing the Ph.D. degree in mechatronic engineering with Beihang University, Beijing, China.

His main research interests are electro-hydraulic servo control and thermal control. His award includes SMC Fellowship of Beihang University.